THE ROLE OF THE PRECIPITATION STRUCTURE ON THE COERCIVITY OF SM(CO,FE,CU,ZR)$_Z$ MAGNETS FOR HT APPLICATIONS

JOSEF FIDLER, THORSTEN MATTHIAS, WERNER SCHOLZ, THOMAS SCHREFL
Vienna University of Technology, Solid State Physics, A-1040 Vienna, Austria
E-mail: fidler@tuwien.ac.at

TIESHENG RONG, IAN P. JONES, I. REX HARRIS
School of Metallurgy and Materials, University of Birmingham, B15 2TT, UK

The magnetic properties of $Sm(Co, Fe, Cu, Zr)_z$ sintered magnets are determined by the cellular precipitation microstructure, which is developed during a complex heat treatment, and by the microchemistry, which is determined by diffusional redistribution processes. The magnetic domain walls are pinned at a continuous $Sm(Co, Cu)_{5-7}$ precipitation structure separating the $Sm_2(Co, Fe)_{17}$ matrix phase. The shape and the thickness of the precipitates and the elemental profiles across them determine the coercivity Hc. The compositional variations across the precipitates are analysed by means of high resolution transmission electron microscopy (FEI Tecnai F20). In addition to the microanalytical investigations numerical micromagnetic simulations were performed in order to show the influence of geometry and size (thickness) of the precipitation structure, the composition and the intrinsic properties, such as the magnetocrystalline anisotropy of the phases on the domain wall pinning behaviour and therefore on the coercivity of various magnets exhibiting sufficiently large coercive field in the high temperature range. Depending on the difference of the magnetocrystalline anisotropy of the precipitation and matrix phases attractive and repulsive domain wall pinning behaviour are distinguished. This work is a combination of microstructural characterisation and micromagnetic simulations and reports on the influence of the heat treatment on the formation of the precipitation structure as well as on the calculated, theoretical limits of the coercive field. TEM images reveal that the microstructures are very similar with cell sizes in the range of 90 to 100 nm. However, the magnetic measurements show that the coercivity is very sensitive on the microchemistry that is influenced by the solutionizing treatment.

1 Introduction

$Sm(Co, Fe, Cu, Zr)_z$ permanent magnets are the best choice for operating temperatures above 300 °C because of the high magnetocrystalline anisotropy, the strong domain wall pinning and the high Curie temperature[1,2,3]. A complex production process, which involves sintering, homogenizing, isothermal aging and annealing, results in the formation of a cellular precipitation structure which acts as pinning centers for magnetic domain walls[4]. The microstructure, which consists of the $Sm_2(Co, Fe)_{17}$ cell matrix phase, the $Sm(Co, Cu)_{5-7}$ cell boundary phase and the Zr-rich lamella phase, develops mainly during the isothermal aging[5]. A numerical micromagnetic model based on the finite element (FE) method was developed in order to analyze the influence of variations of the microstructure as well as of the microchemistry on the coercive field. The micromagnetic model consists of 2x2x2 cells with a cell diameter of 125 nm (fig. 1), which is consistent with measurements from transmission electron microscopy (TEM). The influence of the cell size on the magnetic properties has been studied previously and it showed a strong increase of coercivity with increasing size of the cells[6].

The formation of a fine cellular precipitation structure is a necessary precondition for high magnetic properties at elevated temperatures, because the precipitates act as pinning centers for the magnetic domain walls. However, the compositions of the distinct phases and the elemental profiles also have an even higher influence on the magnetic properties.

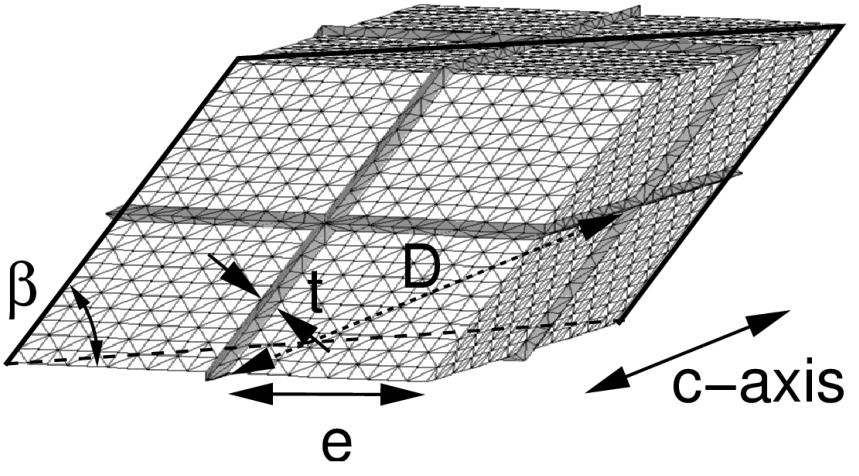

Figure 1. Finite element model of 2x2x2 cells with a cell diameter D=125 nm and a variable cell boundary thickness t.

The diffusional redistribution of the various elements during the heat treatment results in a characteristic microchemistry. As all of the elements are placed on regular crystallographic sites there is only diffusion of vaccancies, which is very slow compared to interstitial diffusion. There are two main diffusional processes: Cu segregates to the 1:5 precipitates and Fe segregates to the 2:17 matrix phase.

As the cell size of the precipitation structure increases with the duration of the isothermal aging, it is necessary to decrease the temperature when the desired cell size has been obtained. Diffusion continues during the following slow cooling and the subsequent annealing at 400 °C but with a reduced rate because of the lower temperatures. Even the solutionized samples may have a microstructure and microchemistry which have a strong influence on the duration and the profile of the heat treatment. Tang et al. reported Cu clusters within the solid solution which enabled a higher Cu diffusion rate and allowed the samples to be quenched directly after the isothermal aging[7].

Analyses of the microchemistry have to be performed in a field emission gun (FEG) TEM, because the spot size of conventional TEMs is too large to focus on the precipitates.

2 Methods

The investigated samples were prepared using the typical powder metallurgy production route, including jetmilling, powder blending and compaction of oriented powder. The production process, using industrial equipment, and the magnetic properties have been recently described[8]. Microstructural analysis was carried out using a JEOLJEM-200CX and a FEI TecnaiF20 200keV transmission electron microscope (TEM) equipped with a field emission gun and an energy dispersive x-ray detector.

3 Results

Several magnets have been analysed by means of TEM and nanoanalytical EDX. Table 1 shows the nominal composition of the analysed magnets.

The samples D and E have an identical composition and have been subjected to an identical precipitation heat treatment, but to different solution heat treatments. Surprisingly,

Table 1. Nominal composition of several magnets: $Sm(Co_{1-a-b-c}Fe_aCu_bZr_c)_z$

Sample	Nominal composition (at.%)		
	Fe	Cu	Zr
A	12.3	6.6	3,1
B	–	11.0	2,3
C	6.3	11.0	2,3
D	12.5	7.7	2,5
E	12.5	7.7	2,5

Table 2. Room temperature magnetic properties of the magnets D and E

	D	E
B_r [T]	0,94	0,8
${}_BH_c$ [kA/m]	333	554
H_K [kA/m]	68	420
${}_iH_c$ [kA/m]	598	> 1500

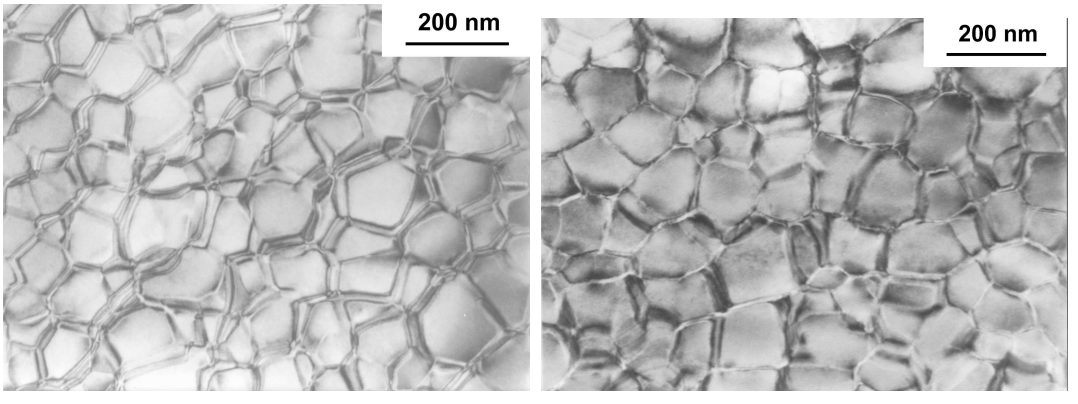

Figure 2. Cellular structures of the magnets D (left) and E (right). The microstructure is very similar, which suggests that the different magnetic properties are related to differences in the microchemistry.

small differences in the solution heat treatment influence enormously the magnetic properties. Table 2 summarizes the magnetic properties of the two samples. The low remanence of sample E is either related to a measurement error or to a bad alignment of the sample. However, the interpolation of the remanences of samples with different Sm content suggests $B_r = 0.92\,\mathrm{T}$.

Figures 2 and 3 show that the cellular and lamellar precipitation structure of both samples is very similar. Therefore it can be concluded that the different magnetic properties result from a different microchemistry. The comparison of the two magnets illustrates nicely that a well developed microstructure is only a necessary precondition for high coercivity, but that the determining factor is the microchemistry. Figure 4 shows a typical EDX linescan across a precipitate of sample E.

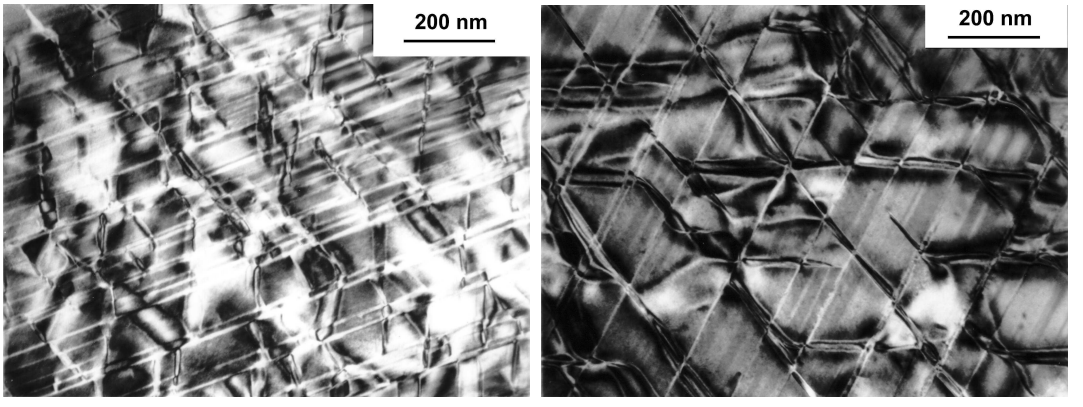

Figure 3. Lamellar structures of the magnets D (left) and E (right)

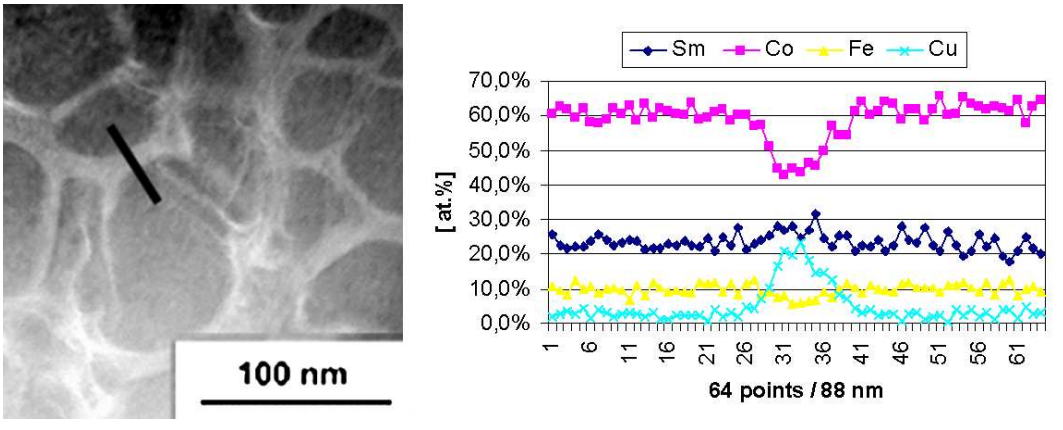

Figure 4. Elemental profiles across a precipitate of sample E.

The microstructure of $Sm(Co, Fe, Cu, Zr)_z$ magnets can be tailored by the Sm content. A higher Sm content results in a higher volume fraction of the cell boundary phase, which, depending on the heat treatment, results either in thicker cell boundaries or in smaller cells. TEM analysis shows that, for an identical heat treatment, generally a smaller cellular structure is formed[9]. However, the micromagnetic simulations show that a thicker cell boundary phase is favorable for a high coercivity (fig. 5). This suggests that, if an improved heat treatment resulted in larger cells with thicker cell boundaries, a higher coercivity could be achieved. A minimum thickness of 10 nm is necessary for a high coercive field of more than 1000 kA/m. However, for very thick intercellular phases, the pinning field decreases again. Figure 6 shows the reason for this behavior in the case of attractive pinning: The domain wall bends into the precipitation phase, which leads to high stray fields at the corners of the cells and facilitates the reversal of magnetization in the cells. For a thickness of more than 40 nm of the intercellular phase, the pinning behavior is lost again, because the domain wall sweeps through the whole intercellular phase and reverses its magnetization. As a result, the unreversed cells remain until nucleation starts the reversal of their magnetization. In the case of repulsive domain wall pinning, a minimum thickness of the intercellular phase is required, too. However, in this regime the pinning field strongly increases for increasing

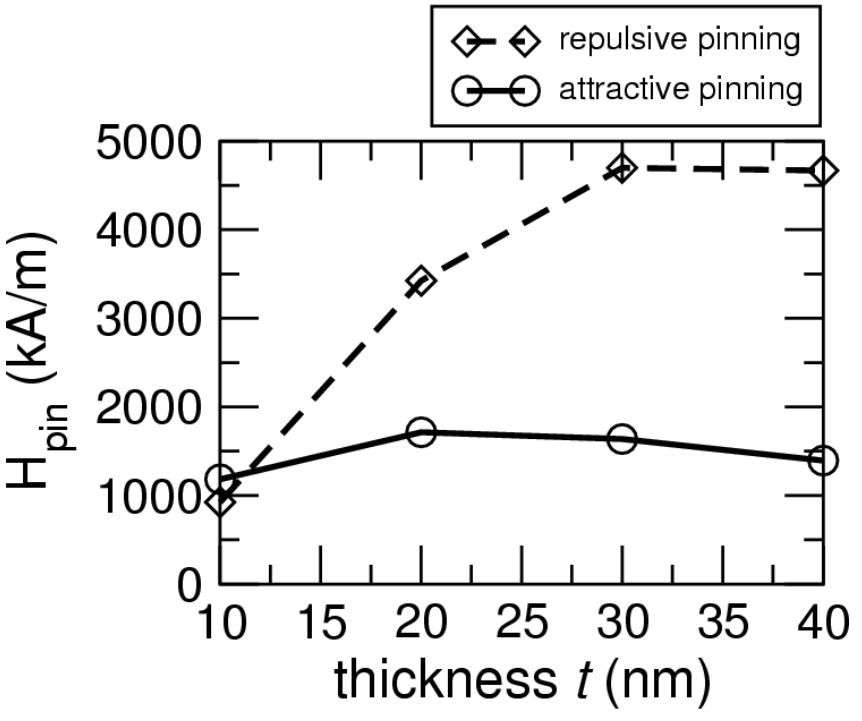

Figure 5. Results of FE simulations: Pinning field vs. thickness of the cell boundary phase for different pinning mechanisms. Attractive pinning leads to lower calculated coercive field values than repulsive pinning.

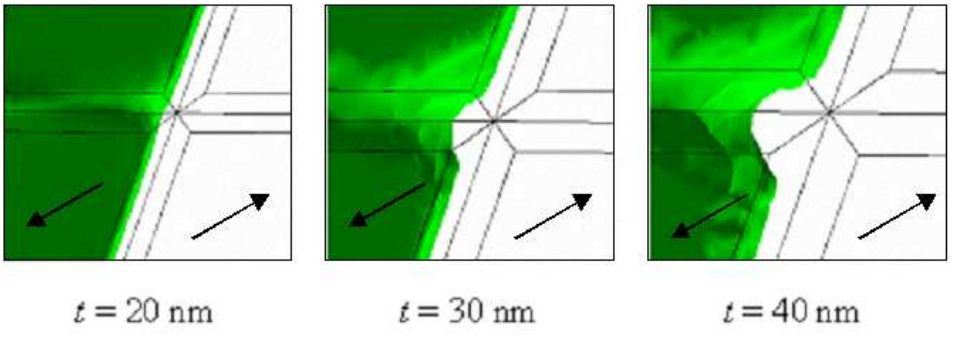

Figure 6. Bending of the domain wall into the intercellular phase (attractive pinning).

thickness until it reaches a maximum level, which is shown in figure 5. Once again, the sharp corners of the cells play an important role, because this is the place where the domain wall can cross the intercellular phase (fig. 7). As the thickness of the intercellular phase increases, the energy barrier becomes wider and this mechanism gets more and more difficult.

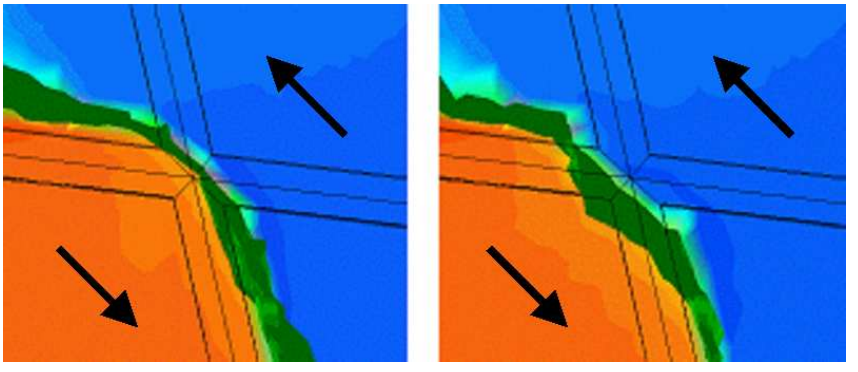

Figure 7. Depinning of the domain wall on the corners of the rhombohedral cells (repulsive pinning).

3.1 The cell matrix phase

Table 3 shows the measured compositions of the cell matrix phases. Additions of Cu decrease the spontaneous magnetisation of the 2:17 phase[10], and should be as low as possible. The Cu content of the cell matrix phase is therefore a good check as to whether the heat treatment has been appropriate for this specific composition or not. An improved heat treatment should decrease the Cu content in this phase and increase the remanence. But this would increase the Cu content in the 1:5 cell boundaries which might, depending on the current Cu content, improve or deteriorate the coercivity. There are two steps to improve the magnetic properties. The first one is to optimise the heat treatment in order to increase the segregation of Cu in the 1:5 precipitates. If the optimal Cu content in the 1:5 phase is reached, then it is necessary to decrease the nominal Cu content and to adjust the heat treatment again, in order to achieve a nearly Cu-free cell matrix phase and a sufficiently high Cu content in the cell boundaries. These two steps may be repeated several times. The minimal measured Cu content of 2 at.% in the sample C gives probably an upper limit for the achievable Cu content in the 2:17 phase. As sample C has a very high nominal Cu content of 11 at.%, it seems reasonable that this is really an upper limit for high temperature magnets with Cu contents below 10 at.%.

The Fe content within the cell matrix phase is always higher than the nominal content, which confirms that Fe mainly segregates to the 2:17 phase. A higher Fe/Co-ratio decreases the anisotropy constant K_1[11] and increases the spontaneous magnetization M_s[12].

The Zr content within the cell matrix phase lies between 1,0 an 2,4 at.%. Because of the low Zr concentration, a detailed analysis would require longer measurement times in order to achieve a better signal to noise ratio. Nevertheless the data reveal that the Zr content within the 2:17 phase is higher than expected[13,14].

3.2 The cell boundary phase

The cellular $Sm(Co, Cu)_{5-7}$ precipitation structure acts as pinning centers for the magnetic domain walls. The coercivity is determined by the difference and the gradient of the domain wall energy. The exchange constant A and the anisotropy constant K_1 of the cell boundary phase are mainly determined by the Cu concentration[15]. The investigations reveal that, in general, the Cu concentration is rather low (tab. 4) resulting in a repulsive pinning coercivity mechanism [16]. The Cu content in the 1:5 phase should be as low as possible or as high as necessary to make the 1:5 phase non-ferromagnetic. In low Cu samples the K_1 values of the 1:5 and the 2:17 phases cross at a certain temperature, which does not happen in high Cu

Table 3. Average composition of the cell matrix phases of several magnets analysed with EDX.

Sample	Average composition of the cell matrix phase (at.%)					
	Fe	±	Cu	±	Zr	±
A	16.7	1.5	2.0	0.8	1.3	1,2
B	–	–	3.9	0.8	1.9	1,3
C	8.1	0.7	2.0	0.4	2.3	0,7
D	13.5	1.3	3.3	0.4	1.0	1,3
E	13.0	0.8	3.5	0.9	2.4	0,6

Table 4. Average composition of the cell boundary phases of several magnets analysed with EDX.

Sample	Average composition of the cell boundary phase (at.%)					
	Fe	±	Cu	±	Zr	±
A	10.8	1.3	12.5	1.2	1.1	1,2
B	–	–	15.6	1.3	2.1	1,4
C	7.2	0.6	9.6	0.6	1.6	0,6
D	5.2	2.9	32.9	10.5	1.4	1,4
E	9.7	1.8	15.8	6.7	2.5	1,2

samples. However, as a large part of the magnet consists of the 1:5 phase, the spontaneous magnetization M_s is strongly decreased in high Cu samples.

The addition of Fe should increase the spontaneous magnetization M_s. Therefore it should segregate to the 2:17 cell matrix phase. The Fe content in the cell boundary phase is therefore, similar to the Cu content in the cell matrix phase, an indicator of the quality of the heat treatment. The Zr content is comparable in the cell boundary and in the cell matrix phase (tab. 3 and 4).

4 Conclusion

The microstructural investigations in combination with the micromagnetic simulations reveal that the magnetic properties of $\mathrm{Sm(Co, Fe, Cu, Zr)}_z$ permanent magnets are strongly related to the microstructure and to the microchemistry. The microstructure can be tailored by the composition and the heat treatment. The heat treatment has to be finely adjusted to the composition because the diffusional redistribution is very sensitive to the heat treatment parameters. The nanoanalytical characterisation of the Cu profiles at the precipitates reveals that the magnetization reversal of the investigated magnets is determined by a repulsive pinnng mechanism.

5 Acknowledgement

This work is supported by the EC project HITEMAG (GRD1-1999-11125).

References

1. Strnat, K. J., Rare earth-cobalt permanent magnets, in "Ferromagnetic Materials", edited by E. P. Wohlfarth and K. H. J. Buschow, North-Holland, 1988, vol. 4, pp. 131-209.
2. C. H. Chen, M. S. Walmer, M. H. Walmer, S. Liu, G. E. Kuhl, G. K. Simon, *$Sm_2(Co, Fe, Cu, Zr)_{17}$ magnets for use at temperature $\geq 400^\circ C$*, J. Appl. Phys. 83 (11), 6706-6708 (1998)
3. G. C. Hadjipanayis, W. Tang, Y. Zhang, S. T. Chui, J, F, Liu, C. Chen, H. Kronmüller, *High temperature 2:17 magnets: relationship of magnetic properties to microstructure and processing*, IEEE Trans. Magn. 36 (5), 3382-3387 (2000)
4. J. Fidler, *Coercivity of precipitation hardened cobalt rare earth 17:2 permanent magnets*, J. Magn. Mag. Mat. 30 (1), 58-70 (1982)
5. J. Fidler, P. Skalicky, F. Rothwarf, *High Resolution Electron Microscope Study of Sm(Co,Fe,Cu,Zr)$_{7,5}$ Magnets*, IEEE Trans. Magn. 19 (5), 2041-2043 (1983)
6. B. Streibl, J. Fidler and T. Schrefl, *Domain wall pinning in high temperature $Sm(Co, Fe, Cu, Zr)_{7-9}$ magnets*, J. Appl. Phys. 87, 4765-4767 (2000)
7. W. Tang, Y. Zhang, D. Goll, G. C. Hadjipanayis, H. Kronmüller, *New $Sm(Co, Fe, Zu, Zr)_z$ magnets with better temperature stability*, J. Magn. Magn. Mat. 226-230, 1365-1366 (2001)
8. D. Schobinger, O. Gutfleisch, D. Hinz, K.-H. Müller, L. Schultz, G. Martinek, *High temperature magnetic properties of 2:17 Sm-Co magnets*, J. Magn. Magn. Mat. (2002) in print
9. T. Matthias, G. Zehetner, J. Fidler, W. Scholz, T. Schrefl, D. Schobinger and G. Martinek, *TEM-analysis of Sm(Co,Fe,Cu,Zr)$_z$ magnets for high temperature applications*, J. Magn. Magn. Mat. (2002) in print
10. H. H. Stadelmaier, E.-T. Heni, G. Schneider, G. Petzow, *The metallurgy of permanent magnets based on $Co_{17}Sm_2$*, Z. Metallkunde, Art.-Nr. 5538/1 (1988)
11. R. S. Perkins, S. Straessler, *Interpretation of the magnetic properties of pseudobinary $Sm_2(Co, M)_{17}$ compounds. I. Magnetocrystalline anisotropy*, Phys. Rev. B 15 (1), 477-489 (1977)
12. R. S. Perkins, S. Straessler, *Interpretation of the magnetic properties of pseudobinary $Sm_2(Co, M)_{17}$ compounds. II. Magnetization*, Phys. Rev. B 15 (1), 490-495 (1977)
13. A. E. Ray, *Metallurgical behavior of $Sm(Co, Fe, Cu, Zr)_z$ alloys*, J. Appl. Phys. 55 (6), 2094-2096 (1984)
14. A. E. Ray, *A revised model for the metallurgical behavior of 2:17 type permanent magnetic alloys*, J. Appl. Phys. 67 (9), 4972-4974 (1990)
15. E. Lectard, C. H. Allibert, R. Ballou, *Saturation magnetization and anisotropy in the $Sm(Co_{1-x}Cu_x)_5$ phases*, J. Appl. Phys. 75 (10), 6277-6279 (1994)
16. W. Scholz, J. Fidler, T. Schrefl, D. Suess and T. Matthias, *Micromagnetic simulation of domain wall pinning in $Sm(Co, Fe, Cu, Zr)_z$ magnets*, J. Magn. Magn. Mat. (2002) in print